

Gatifloxacin inducing apoptosis of stromal fibroblasts through cross-talk between caspase-dependent extrinsic and intrinsic pathways

Bin Xu, Yun-Long Sui, Ting-Jun Fan

Laboratory for Corneal Tissue Engineering, College of Marine Life Sciences, Ocean University of China, Qingdao 266003, Shandong Province, China

Correspondence to: Ting-Jun Fan. Laboratory for Corneal Tissue Engineering, College of Marine Life Sciences, Ocean University of China, Qingdao 266003, Shandong Province, China. tjfan@ouc.edu.cn

Received: 2018-08-13 Accepted: 2019-07-11

Abstract

• **AIM:** To reveal the cytotoxicity and related mechanisms of gatifloxacin (GFX) to stromal fibroblasts (SFs) *in vitro*.

• **METHODS:** SFs were treated with GFX at different concentrations (0.009375%-0.3%), and their viability was detected by MTT method. The cell morphology was observed using light/transmission electron microscope. The plasma membrane permeability was measured by AO/EB double-staining. Then cell cycle, phosphatidylserine (PS) externalization, and mitochondrial transmembrane potential (MTP) were analyzed by flow cytometry. DNA damage was analyzed by electrophoresis and immunostaining. ELISA was used to evaluate the caspase-3/-8/-9 activation. Finally, Western blotting was applied for detecting the expressions of apoptosis-related proteins.

• **RESULTS:** Morphological changes and reduced viability of GFX-treated SFs demonstrated that GFX above 0.009375% had cytotoxicity to SFs with dependence of concentration and time. GFX-treating cells also showed G₁ phase arrest, increased membrane permeability, PS externalization and DNA damage, which indicated that GFX induced apoptosis of SFs. Additionally, GFX could activate the caspase-8, caspase-9, and caspase-3, induce MTP disruption, downregulate B-cell leukemia-2 (Bcl-2) and B-cell leukemia-XL (Bcl-XL), and upregulate Bcl-2 associated X protein (Bax), Bcl-2-associated death promoter (Bad), Bcl-2 interacting domain (Bid) and cytoplasmic cytochrome C in SFs, suggesting that caspase-dependent extrinsic and intrinsic pathways were related to GFX-contributed apoptosis of SFs.

• **CONCLUSION:** The cytotoxicity of GFX induces apoptosis of SFs through triggering the caspase-dependent extrinsic and intrinsic pathways.

• **KEYWORDS:** gatifloxacin; stromal fibroblasts; cytotoxicity; apoptosis; caspase; extrinsic pathway; intrinsic pathway

DOI:10.18240/ijo.2019.10.02

Citation: Xu B, Sui YL, Fan TJ. Gatifloxacin inducing apoptosis of stromal fibroblasts through cross-talk between caspase-dependent extrinsic and intrinsic pathways. *Int J Ophthalmol* 2019;12(10):1524-1530

INTRODUCTION

Bacterial keratitis is a very common ocular infection and the main reason causing ocular morbidity and blindness. Whereas, approximately 72% of infections can be successfully cured topically with appropriate antibiotics^[1]. Fluoroquinolones, as bactericidal antibiotics, are broadly applied for bacterial keratitis because of their wide spectrum of activity and their effectiveness against multidrug resistant organisms^[2]. Fourth-generation products of ophthalmic fluoroquinolones have been developed. Gatifloxacin (GFX; 2003), one of newer fourth-generation fluoroquinolones, has been approved in eye disease treatments in clinical. The most important feature of the fourth-generation fluoroquinolones is their improved Gram-positive activity by targeting both DNA gyrase and topoisomerase IV of bacterial cells in a balanced fashion, different from the early-generation agents^[3], and other potentially beneficial characteristics include improved drug delivery into the anterior segment of the eye, enhanced activity against certain strains of atypical mycobacteria and lowered likelihood of selecting for resistant bacterial strains^[4].

For treatment of bacterial keratitis, both efficacy and side-effect of antibiotics should be taken into account^[5]. Recently, GFX has been reported that it affects the viability of corneal epithelial cells and corneal epithelial wound healing^[6-8]. Due to ocular well penetration for fluoroquinolones^[9-10], GFX might have negative effects on stromal keratocytes^[11-12]. GFX displays the potential cytotoxic effects to keratocytes, depending on drug concentrations and duration of exposure^[13]. However, the cytotoxic mechanisms of GFX to keratocytes has not been fully elucidated.

Moreover, keratocytes are quiescent and can transform into repair-phenotype of activated stromal fibroblasts (SFs) following injury and keratoplasty^[14]. The activated SFs become more

susceptible to drug treatment. Unfortunately, few attentions have been paid to the cytotoxic effects of GFX to SFs of the exposed corneal stroma, especially after cornea surgery. Therefore, we established an SF cell model *in vitro* using activated human corneal stromal (HCS) cells cultured with fetal bovine serum (FBS)^[15], to explore the cytotoxicity of GFX and its potential mechanisms for prospective therapeutic interventions in eye clinics^[16-17].

MATERIALS AND METHODS

Cell Culture and Reagents SFs, an established non-transfected HCS cell line^[18], were cultured in DMEM/F12 medium (Gibco, Rockville, MD, USA) containing 10% FBS (Gibco) at 37°C in a moist atmosphere with 5% CO₂. GFX (C₁₉H₂₂FN₃O₄) was purchased from Sigma-Aldrich (St. Louis, MO, USA). A stock solution was prepared at a concentration of 0.6% (2-fold its clinical therapeutic dosage of 0.3%) by dissolving GFX in 10% FBS-DMEM/F12 medium. The stock solution was serially diluted with the same medium to final concentrations from 0.3% to 0.009375%. The 3-[4,5-dimethylthiazol-2-yl]-2, 5 diphenyltetrazolium bromide (MTT) powder, dimethyl sulfoxide, acridine orange (AO), ethidium bromide (EB), 5,5',6,6'-tetrachloro-1,1',3,3'-tetraethylbenzimidazolylcarbocyanineiodide (JC-1) were obtained from Sigma-Aldrich. γ H2A.X antibody and FITC-labeled secondary antibody were obtained from Abcam (Cambridge, UK). PI and RNase solution was obtained from BD Biosciences (San Jose, CA, USA). RIPA Lysis Buffer was obtained from Biotime Company (Shanghai, China). All primary antibodies and horseradish peroxidase (HRP)-conjugated secondary antibodies for ELISA and western blotting were obtained from Proteintech (Rosemont, IL, USA).

GFX Treatment SFs were seeded into various specifications of culture plates (Nunc, Copenhagen, Denmark). After cells grew about 70% confluence, the medium was replaced entirely with fresh medium containing GFX at concentrations ranging from 0.009375% to 0.3%, respectively. SFs were as blank controls in all experiments that were cultured in fresh 10% FBS-DMEM/F12 medium without GFX. Cell morphology and growth status were observed under an Eclipse TS100 inverted light microscope (Nikon, Tokyo, Japan) per 4h.

MTT Assay MTT assay was performed to assess cell viability of SFs as previously described^[19]. Briefly, SFs were cultured in 96-well plates (2×10⁴ cells per well) and treated with GFX as described above. Then, 20 μ L of 5 mg/mL MTT was added into each well and incubated at 37°C in dark for 4h. After discarding the medium, 150 μ L of dimethyl sulfoxide was added, and then their absorbance values were measured using a Multiskan GO microplate reader at 490 nm (Thermo Scientific, MA, USA).

Transmission Electron Microscopy The ultrastructure of SFs was obtained by transmission electron microscopy (TEM)

as previously described^[20]. In brief, the cells cultured in 6-well plates (approximately 1.5×10⁶ cells per well) were treated with 0.15% GFX and harvested at 4h intervals. After successive fixation with 4% glutaraldehyde and 1% osmium tetroxide, SFs were dehydrated and embedded in epoxy resin. After staining with 2% uranyl acetate and lead citrate, ultrathin sections were assessed by an H700 TEM (Hitachi, Tokyo, Japan).

AO/EB Double Staining AO/EB double-staining was conducted to measure the plasma membrane permeability of SFs as previously reported^[20]. In brief, SFs were seeded into 24-well plates (approximately 1×10⁵ cells per well), and treated with GFX as described above. Cells were harvested after digestion with 0.25% trypsin and centrifugation (200 g, 10min), and stained by 100 μ g/mL AO/EB (1:1) solution for 1min. The stained cells were observed using a Nikon Ti-S fluorescent microscope; the apoptotic cells were with red or orange nuclei and counted, while cells with green nuclei were non-apoptotic. At least 400 cells were counted in each group from three parallel wells, and the apoptotic ratio was calculated by the equation "apoptotic ratio (%) = number of apoptotic cells/total number of cells × 100".

DNA Damage Detection The DNA fragmentation of SFs was analyzed by Agarose gel electrophoresis as previously described^[19] and modified. Briefly, SFs cultured in 6-well plates (approximately 1.5×10⁶ cells per well) were treated with GFX and collected as described above. After washing with ice-cold PBS and centrifugation (200 g, 10min), their DNA was extracted using TIANamp Genomic DNA Kit (Tiangen Biotech, Beijing, China). DNA were electrophoresed on 1.5% agarose gel at 150 V for 40min. Then the gel was photographed and analyzed using an UVP EC3 imaging system (Upland, CA, USA) after staining with ethidium bromide. In addition, γ H2A.X, an early marker of DNA damage, were measured by immunocytochemistry analysis. Briefly, cells cultured in 24-well plate were fixed in 4% paraformaldehyde, blocked with 5% bovine calf serum, and permeabilized with 0.1% Triton-X. Then the cells were incubated with the primary antibody (1:500) for 2h at 37°C and FITC-labeled goat anti-rabbit secondary antibody (1:2000) for 1h at room temperature in order. Finally, the cells were counterstained with DAPI for 10min and observed under a Nikon Ti-S fluorescent microscope.

Flow Cytometry Analysis We further performed flow cytometry (FCM) assay to analyze cell cycle, phosphatidylserine (PS) orientation, and mitochondrial transmembrane potential (MTP), as previously reported^[19]. Briefly, SFs cultured in 6-well plates (approximately 1.5×10⁶ cells per well) were treated and harvested per 4h as described above, and fixed with cold 70% alcohol overnight at 4°C. For cell cycle assay, 5 μ L

of 5 mg/mL PI and RNase solution was added into 500 μ L of fixed cell suspension, and reacted in dark for 30min. For PS externalization assay, 5 μ L FITC-Annexin V and 5 μ L PI were added into 500 μ L of cell suspension using FITC-Annexin V Apoptosis Detection Kit I (BD Biosciences), and incubated in dark for 15min. For MTP assay, 5 μ L of 10 μ g/mL JC-1 solution was added into 500 μ L cell suspension, and reacted in dark for 15min. The stained cells were detected and analyzed by a FACS can flow cytometer using the CXP analysis software (BD Biosciences).

ELISA Detection ELISA was used to measure caspase activation in SFs as previously described^[20] and modified. Briefly, SFs inoculated in 6-well plates (approximately 1.5×10^6 cells per well) were treated and collected every 2h as described above. Whole-cell protein were extracted using 500 μ L of RIPA lysis buffer containing PMSF following manufacturer's instructions. The 100 μ L protein extract was coated onto a 96-wells ELISA plate (Nunc), followed by blocking with 5% non-fat milk, incubated with 100 μ L of rabbit anti-human caspase-3, -8, and -9 (active forms) monoclonal antibodies (1:1000), respectively, at 37°C for 90min. After washing with 0.05% PBST (5min \times three times), then incubated with HRP-conjugated goat anti-rabbit secondary antibody (1:2000) at 37°C for 120min, the wells were washed with 0.05% PBST solution (5min \times three times), added 1% TMB and reacted at room temperature in dark for 25min. After color developing, the reaction was stopped with 50 μ L of 0.5 mol/L H₂SO₄ solution, their absorbance values at 490 nm were measured by a Multiskan GO microplate reader (Thermo Scientific).

Western Blot Analysis Western blotting was performed to quantify expression levels of apoptosis-related proteins in GFX-treated SFs, as previously described^[21]. Briefly, cells cultured in 6-well plate (approximately 1.5×10^6 cells per well) were treated with GFX and harvested per 4h as described above. Total proteins were extracted using RIPA lysis buffer as described above; cytoplasmic proteins were extracted to analyze the mitochondrion-released apoptosis-triggering proteins using the mitochondrion/cytoplasmic protein extraction kit (Sangon biological engineering, Shanghai, China) following manufacturer's instructions. Equal amounts of protein were separated by 10% SDS-PAGE, and transferred onto PVDF membranes. After blocking with 5% non-fat milk, the membranes were incubated with rabbit anti-human IgG monoclonal antibody targeting β -actin (1:5000), B-cell leukemia-2 (Bcl-2, 1:1000), B-cell leukemia-XL (Bcl-XL, 1:500), Bcl-2 associated X protein (Bax, 1:2000), Bcl-2-associated death promoter (Bad, 1:500), Bcl-2 interacting domain (Bid, 1:500) and cytochrome C (1:5000), respectively for 120min at 37°C. Next, incubated with HRP-conjugated goat anti-rabbit IgG monoclonal antibody (1:2000) for 90min

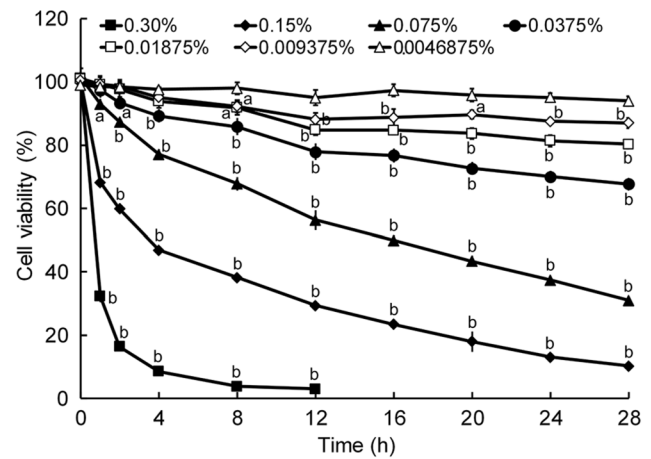


Figure 1 Reduced viability of GFX-treated SFs MTT assay for SF cell viability after exposure to GFX at different concentrations and different times. Cell viability was presented as percentage (mean \pm SD) compared with that of the corresponding blank control according to absorbance value at 490 nm ($n=3$). ^a $P<0.05$ and ^b $P<0.01$ vs blank control.

at 37°C. Then, washed with 0.05% TBST solution for 5min, three times. The signal was developed using an enhanced chemiluminescent (ECL) detection kit (Pierce, Rockford, IL, USA) and observed with Tanon 5200 system (Shanghai, China). Optical density of each band was analyzed with the ImageJ 1.48 image analysis software (NIH, NY, USA), in which β -actin was considered as an internal control.

Statistical Analysis Each experiment was repeated three times independently. Measurement data were expressed as mean \pm standard deviation (SD) and were analyzed by one-way ANOVA and unpaired Dunnett's *t*-test assuming equal variance, with the SPSS 22.0 software (SPSS Inc., Chicago, IL, USA). P values <0.05 was considered statistically significant.

RESULTS

GFX Exhibits Cytotoxicity to Stromal Fibroblasts To investigate the cytotoxicity of GFX to SF cell viability, firstly, we conducted MTT assay. The results showed that the viability of SFs significantly declined with concentration and time after treatment with GFX at concentrations of 0.009375% and above ($P<0.01$ or 0.05), while SFs exposed to 0.0046875% GFX had no significant difference compared with that of blank control (Figure 1).

Then we observed the abnormal alterations of growth status and morphology of SFs in different groups. The growth inhibition and cytopathic morphological alterations (such as cellular atrophy) were observed with dependence of concentration and time after treatment with GFX at concentrations varying from 0.3% to 0.0375%, while there was no significant difference between the 0.01875% GFX and blank control groups (Figure 2A). Moreover, TEM results revealed that 0.15% GFX-treated SFs exhibited ultrastructure abnormalities, including mitochondrion swelling, cytoplasmic vacuolation, chromatin condensation,

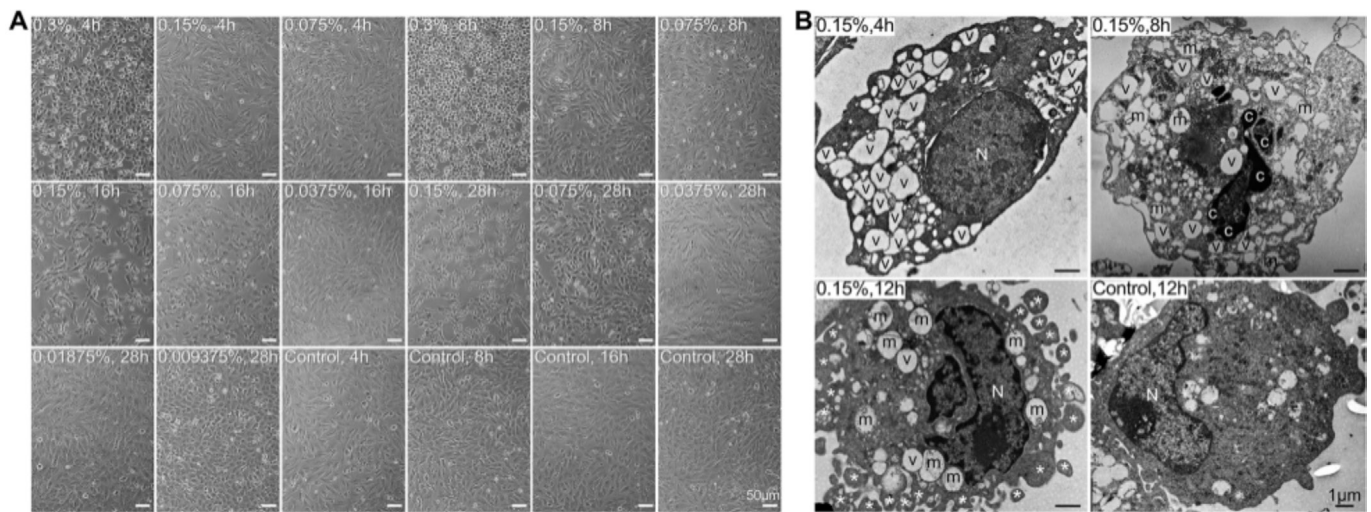


Figure 2 Morphological changes of GFX-exposed SFs A: Light microscopy results showed GFX-induced cellular atrophy and growth retardation. Scale bar, 50 μm; B: TEM showed cytoplasmic vacuolation (v), swollen mitochondrion (m), condensed chromatin (c), and suspected apoptotic bodies (asterisk) of 0.15% GFX-treated SFs. N: Nucleus. Concentrations and exposure time points of GFX were showed at the top-left of each panel. Scale bar, 1 μm.

and suspected apoptotic bodies with the prolongation of treatment time (Figure 2B).

GFX Induced G₁ Phase Arrest of Stromal Fibroblasts To investigate whether the GFX could influence the cell cycle, we used FCM analysis. The results showed that the cell numbers in G₁ phase increased by approximately 28% ($P<0.01$) at 4h, approximately 40% ($P<0.01$) at 8h, and approximately 52% ($P<0.01$) at 12h, respectively, while obviously decreased in S and G₂/M phases ($P<0.01$ or 0.05) over time in 0.15% GFX-treated group, compared with the corresponding blank control (Table 1).

GFX Had Pro-apoptotic Effects on Stromal Fibroblasts AO/EB double staining was conducted to explore the toxicology mechanism of GFX to the SFs. And our results indicated that 0.0375% GFX and above induced the increase of membrane permeability with dependence of concentration and time ($P<0.01$ or 0.05) compared with blank control. The apoptotic rates of SFs in all groups are indicated in Figure 3A. Moreover, the amounts of Annexin V-positive cells after exposure to 0.15% GFX, increased by approximately 46% ($P<0.01$) at 4h, approximately 59% ($P<0.01$) at 8h, and approximately 68% ($P<0.01$) 12h, compared with that of blank control, respectively (Figure 3B). Agarose gel electrophoresis showed that the genomic DNA were highly fragmented with typical DNA ladders in the groups treated with 0.15% and 0.075% GFX at 28h, respectively, while no DNA ladder was shown in the blank control (Figure 3C). Additionally, the fluorescence intensity of positively immunostained with γH2A.X increased in 0.15% GFX-treated SFs from 4h to 28h in a time-dependent manner (Figure 3D). Above findings demonstrated that GFX caused DNA damage and apoptosis of SFs.

Table 1 Cell cycle parameters of 0.15% GFX-treated SFs %

Groups	No. of cells		
	G ₁ phase	S phase	G ₂ /M phase
0h	50.75±1.04	26.06±0.46	23.19±0.61
Blank control			
4h	40.93±0.23	27.93±1.12	31.14±1.12
8h	33.01±0.74	30.93±1.18	36.07±0.90
12h	29.52±0.20	31.62±0.76	38.87±0.88
0.15% GFX			
4h	68.67±1.85 ^b	23.28±1.41 ^a	8.06±0.48 ^b
8h	73.17±2.47 ^b	17.26±0.83 ^b	9.57±0.37 ^b
12h	81.74±2.79 ^b	8.92±0.91 ^b	9.34±1.35 ^b

Assayed by flow cytometry by PI staining. The cell numbers of each cell cycle phase were presented as percentage (mean±SD) of the total number of cells ($n=3$). ^a $P<0.05$ and ^b $P<0.01$ vs blank control.

GFX Induced Caspase-dependent Apoptosis of Stromal Fibroblasts To investigate the involved apoptosis pathway inducing by GFX, we carried out the ELISA assay. As shown in Figure 4, caspase-8 was significantly activated from 6 to 14h ($P<0.01$ or 0.05), caspase-9 from 2 to 14h ($P<0.01$ or 0.05), and caspase-3 from 4 to 14h ($P<0.01$ or 0.05) in SFs treated with 0.15% GFX, compared with that of blank control, respectively, in which caspase-8 activation rate peaked at 10h ($P<0.01$), caspase-9 at 6h ($P<0.01$) and caspase-3 at 10h ($P<0.01$).

GFX Induced MTP Disruption and Altered Expressions of Apoptosis-related Proteins FCM results suggested that GFX caused a time-dependent MTP disruption of SFs, and the amounts of JC-1 positive cells increased by approximately 17% ($P<0.01$), approximately 27% ($P<0.01$), and approximately 53% ($P<0.01$) after exposure to 0.15%

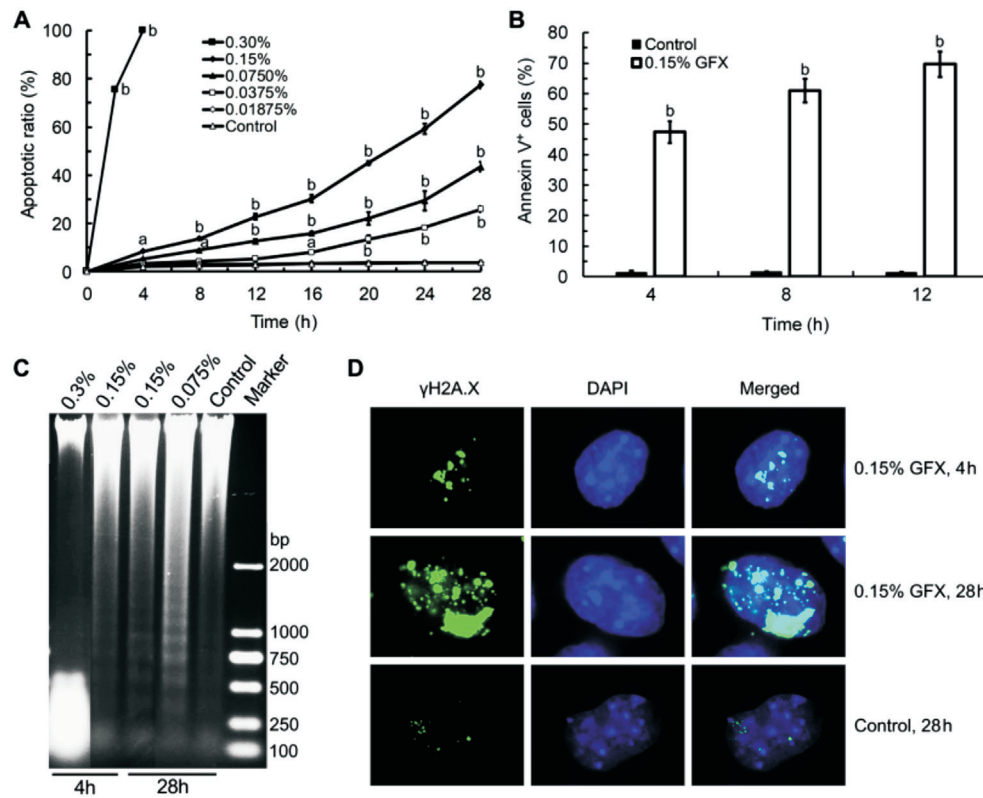


Figure 3 Membrane permeability, PS externalization and DNA damage of GFX-treated SFs. A: AO/EB double staining. The apoptotic ratio of SFs was presented as percentage (mean±SD) of total cell number according to the membrane permeability elevation ($n=3$). B: Flow cytometry assay with Annexin V/PI staining. The number of Annexin V-positive cells, *i.e.* PS externalized cells, was presented as percentage (mean±SD) of total cell number ($n=3$). C: DNA electrophoresis. Genomic DNA of cells treated with or without GFX was electrophoresed, and DNA bands were shown; D: 0.15% GFX-treated SFs showed immunostaining patterns for γ -H2A.X in time-dependent manner. ^a $P<0.05$ and ^b $P<0.01$ vs blank control.

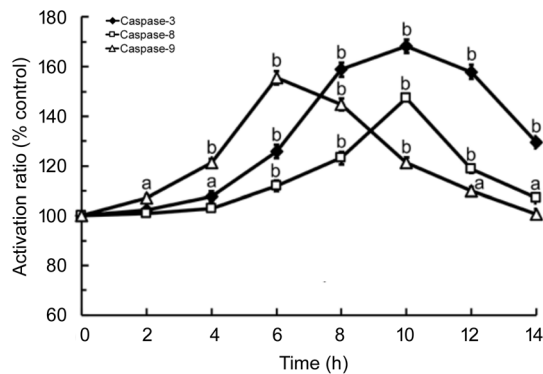


Figure 4 Caspase activation of 0.15% GFX-treated SFs. The activation ratios of caspase-3, -8 and -9 were presented as percentage (mean±SD) compared with the corresponding blank control based on 490 nm absorbance ($n=3$). ^a $P<0.05$ and ^b $P<0.01$ vs blank control.

GFX for 4, 8, and 12h, compared with that of blank control, respectively (Figure 5A). Western blot results indicated that GFX downregulated the expression levels of Bcl-2 and Bcl-XL ($P<0.01$), and upregulated Bax, Bad and Bid ($P<0.01$) with dependence of time after exposure to 0.15% GFX for 4, 8, and 12h. Moreover, GFX also promoted the release of cytochrome C from the mitochondrion, and increased the cytoplasmic accumulation of cytochrome C (Figure 5B and 5C).

DISCUSSION

GFX eye drop is one of most common drugs for treating bacterial keratitis, pre- and postoperative control of infection during keratoplasty^[9]. Unfortunately, there are some reports that claimed it showed toxicity to corneal cells^[7-8,13,22], and its cytotoxic effects remains unclear. So, in this study, we investigated the cytotoxicity of GFX to SFs and its possible mechanisms *in vitro* to provide a therapeutic intervention for bacterial keratitis. The cell viability and morphology are main indices for cytotoxicity evaluation of chemicals and drugs^[15,20]. GFX obviously decreased the viability of SFs with dependence of concentration and time, and also caused dramatic morphological changes of SFs, including cell shrinkage, mitochondrion swelling, chromatin condensation and suspected apoptotic bodies, basically in accordance with the results of cell viability. The results demonstrate that GFX has significant cytotoxicity to SFs at concentrations above 0.009375%. Moreover, cell cycle analysis implies that GFX might induce the growth inhibition of SFs by causing G₁ phase arrest. Based on the cytotoxicity and G₁ phase arrest, we consider that GFX may have pro-apoptotic effects on SFs, which is accordance with previous studies^[23-24].

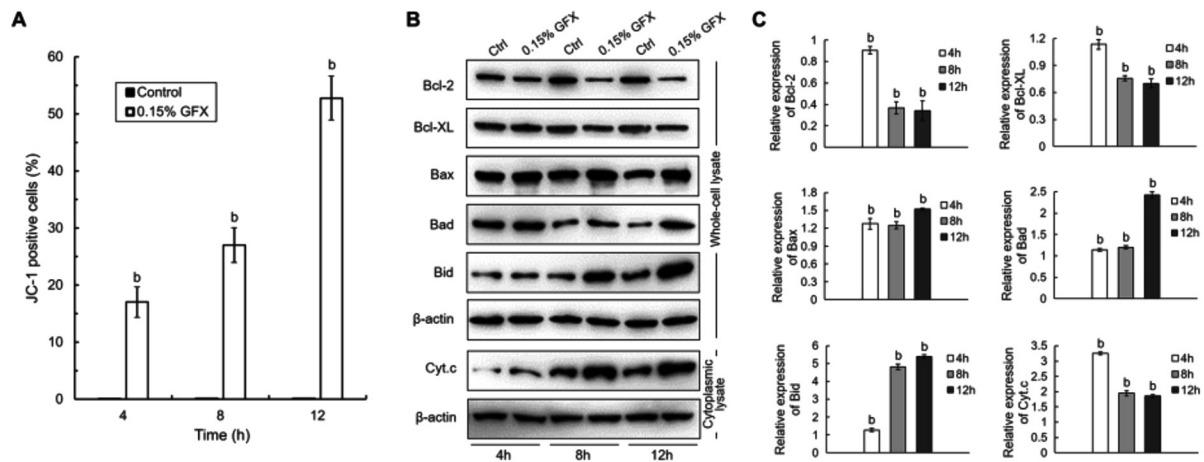


Figure 5 MTP disruption and expression alteration of apoptosis-triggering proteins of 0.15% GFX-treated SFs A: Flow cytometry assay with JC-1 staining. The amounts of JC-1 positive cells, *i.e.* MTP disrupted cells, were presented as percentage (mean±SD) of total cell number ($n=3$). B: Western blot images. Alterations of expression levels of Bcl-2 family proteins along with the cytoplasmic amounts of mitochondria-released cytochrome C are shown. C: Relative densitometric analysis of protein bands by comparing with the expression of β -actin. The relative amounts of each protein were presented as the percentage (mean±SD) of protein band density compared to the corresponding internal control ($n=3$). Cyt. c: Cytochrome C. ^b $P<0.01$ vs blank control.

Then the GFX-induced apoptosis was assessed in SFs. As shown, GFX-treated SFs exhibited the typical characteristics of cell apoptosis, including membrane permeability, PS externalization, and DNA ladder^[21,25]. Our findings imply that GFX contributes to cytotoxicity most probably by inducing apoptosis^[23,26]. Based on above findings, subsequent experiments were conducted to further confirm underlying apoptotic pathways including extrinsic and intrinsic pathways. The extrinsic pathway is mediated by death receptors that cause the autocleavage of pro-caspase-8^[27]. The cleaved caspase-8 as a major initiator caspase can activate downstream effector caspase-3 that is known as a key executor caspase in the apoptosis pathways. After activation of caspase-3, PARP, as the substrate of caspase-3, is cleaved into two fragments, p89 and p24, contributing to DNA fragmentation, resulting in the execution of extrinsic apoptosis^[28-29]. Our findings showed that GFX could activate caspase-8 and caspase-3, suggesting that the extrinsic pathway was involved in the apoptosis of SFs. However, further research is needed to confirm which death receptor mediates the GFX-induced apoptosis of SFs.

Bcl-2 family, classified as anti-apoptotic and pro-apoptotic members, plays an important role in the regulation of the initiation of intrinsic (mitochondrial-mediated) apoptosis^[30-31]. The anti-apoptotic subfamily, including Bcl-2, Bcl-XL, *etc.*, prevents the release of mitochondria-sequestered pro-apoptotic regulators into cytoplasm, while the pro-apoptotic subfamily, such as Bax, Bad, *etc.* induces pro-apoptotic regulators release into the cytoplasm^[32-33]. Moreover, due to MTP disrupting, cytochrome C is released from mitochondria into cytoplasm, which activates key initiator caspase-9 and subsequent downstream effector caspases-3, leading to intrinsic

apoptosis^[34]. Our results demonstrated that GFX could induce the upregulation of Bax and Bad as well as the downregulation of Bcl-2 and Bcl-XL of SFs. The rising ratio of pro-apoptotic proteins induced MTP disruption. And GFX also increased the cytochrome C amounts in cytoplasm, which activated caspase-9 and caspase-3, resulting in executing intrinsic apoptosis. Additionally, active caspase-8 can also induce activation of Bid, a member of Bcl-2 family. The truncated Bid (tBid, active Bid) binds to the pro-apoptotic protein Bax, causing the MTP disruption and the release of cytochrome C^[35]. This result was also found in this study, suggesting that the extrinsic pathway interconnects with the intrinsic pathway, ultimately resulting in caspase-3 activation in the process of apoptosis induction. GFX shows cytotoxicity to SFs with dependence of concentration and time, and induces apoptosis through cross-talk between the caspase-dependent extrinsic and intrinsic pathways. Our findings shine a light on the cytotoxicity and mechanisms of GFX, and provide relevant references for prospective therapeutic interventions in eye clinics.

ACKNOWLEDGEMENTS

The authors would like to thank Prof. Ming-Zhuang Zhu of Key Laboratory of Mariculture, Ocean University of China, for help and guidance in flow cytometry analysis.

Foundation: Supported by the National High Technology R&D Program of China (No.2006AA02A132).

Conflicts of Interest: Xu B, None; Sui YL, None; Fan TJ, None.

REFERENCES

1 Fong CF, Tseng CH, Hu FR, Wang IJ, Chen WL, Hou YC. Clinical characteristics of microbial keratitis in a university hospital in Taiwan. *Am J Ophthalmol* 2004;137(2):329-336.

- 2 Smith A, Pennefather PM, Kaye SB, Hart CA. Fluoroquinolones: place in ocular therapy. *Drugs* 2001;61(6):747-761.
- 3 Mah FS. Fourth-generation fluoroquinolones: new topical agents in the war on ocular bacterial infections. *Curr Opin Ophthalmol* 2004;15(4):316-320.
- 4 Hwang DG. Fluoroquinolone resistance in ophthalmology and the potential role for newer ophthalmic fluoroquinolones. *Surv Ophthalmol* 2004;49(Suppl 2):S79-S83.
- 5 Tsai TH, Chen WL, Hu FR. Comparison of fluoroquinolones: cytotoxicity on human corneal epithelial cells. *Eye (Lond)* 2010;24(5):909-917.
- 6 Burka JM, Bower KS, Vanroekel RC, Stutzman RD, Kuzmowych CP, Howard RS. The effect of fourth-generation fluoroquinolones gatifloxacin and moxifloxacin on epithelial healing following photorefractive keratectomy. *Am J Ophthalmol* 2005;140(1):83-87.
- 7 Sosa AB, Epstein SP, Asbell PA. Evaluation of toxicity of commercial ophthalmic fluoroquinolone antibiotics as assessed on immortalized corneal and conjunctival epithelial cells. *Cornea* 2008;27(8):930-934.
- 8 Oum BS, Kim NM, Lee JS, Park YM. Effects of fluoroquinolone eye solutions without preservatives on human corneal epithelial cells *in vitro*. *Ophthalmic Res* 2014;51(4):216-223.
- 9 Fukuda M, Yamada M, Kinoshita S, Inatomi T, Ohashi Y, Uno T, Shimazaki J, Satake Y, Maeda N, Hori Y, Nishida K, Kubota A, Nakazawa T, Shimomura Y. Comparison of corneal and aqueous humor penetration of moxifloxacin, gatifloxacin and levofloxacin during keratoplasty. *Adv Ther* 2012;29(4):339-349.
- 10 Sharma C, Biswas NR, Ojha S, Velpandian T. Comprehensive evaluation of formulation factors for ocular penetration of fluoroquinolones in rabbits using cassette dosing technique. *Drug Des Devel Ther* 2016;10:811-823.
- 11 Seitz B, Hayashi S, Wee WR, LaBree L, McDonnell PJ. *In vitro* effects of aminoglycosides and fluoroquinolones on keratocytes. *Invest Ophthalmol Vis Sci* 1996;37(4):656-665.
- 12 Leonardi A, Papa V, Fregona I, Russo P, De Franchis G, Milazzo G. *In vitro* effects of fluoroquinolone and aminoglycoside antibiotics on human keratocytes. *Cornea* 2006;25(1):85-90.
- 13 Bezwada P, Clark LA, Schneider S. Intrinsic cytotoxic effects of fluoroquinolones on human corneal keratocytes and endothelial cells. *Curr Med Res Opin* 2008;24(2):419-424.
- 14 Fini ME, Stramer BM. How the cornea heals: cornea-specific repair mechanisms affecting surgical outcomes. *Cornea* 2005;24(8 Suppl):S2-S11.
- 15 Roux SL, Borbely G, Słoniecka M, Backman LJ, Danielson P. Transforming growth factor beta 1 modulates the functional expression of the neurokinin-1 receptor in human keratocytes. *Curr Eye Res* 2016;41(8):1035-1043.
- 16 Lapalus P, Ettaiche M, Fredj-Reygrobelle D, Jambou D, Elena PP. Cytotoxicity studies in ophthalmology. *Lens Eye Toxic Res* 1990;7(3-4):231-242.
- 17 Zorn-Kruppa M, Tykhonova S, Belge G, Diehl HA, Engelke M. Comparison of human corneal cell cultures in cytotoxicity testing. *ALTEX* 2004;21(3):129-134.
- 18 Fan TJ, Hu XZ, Zhao J, Niu Y, Zhao WZ, Yu MM, Ge Y. Establishment of an untransfected human corneal stromal cell line and its biocompatibility to acellular *Porcine corneal stroma*. *Int J Ophthalmol* 2012;5(3):286-292.
- 19 Zhao J, Qiu Y, Tian CL, Fan TJ. The cytotoxic and pro-apoptotic effects of phenylephrine on corneal stromal cells via a mitochondrion-dependent pathway both *in vitro* and *in vivo*. *Exp Toxicol Pathol* 2016;68(7):409-417.
- 20 Shan M, Fan TJ. Cytotoxicity of carteolol to human corneal epithelial cells by inducing apoptosis via triggering the Bcl-2 family protein-mediated mitochondrial pro-apoptotic pathway. *Toxicol In Vitro* 2016;35:36-42.
- 21 Tian CL, Wen Q, Fan TJ. Cytotoxicity of atropine to human corneal epithelial cells by inducing cell cycle arrest and mitochondrion-dependent apoptosis. *Exp Toxicol Pathol* 2015;67(10):517-524.
- 22 Kovoora TA, Kim AS, McCulley JP, Cavanagh HD, Jester JV, Bugde AC, Petroll WM. Evaluation of the corneal effects of topical ophthalmic fluoroquinolones using *in vivo* confocal microscopy. *Eye Contact Lens* 2004;30(2):90-94.
- 23 Fan WY, Sui YL, Fan TJ. Proparacaine induces cytotoxicity and mitochondria-dependent apoptosis in corneal stromal cells both *in vitro* and *in vivo*. *Toxicol Res (Camb)* 2016;5(5):1434-1444.
- 24 Wen Q, Fan TJ, Tian CL. Cytotoxicity of atropine to human corneal endothelial cells by inducing mitochondrion-dependent apoptosis. *Exp Biol Med (Maywood)* 2016;241(13):1457-1465.
- 25 Takemura G, Kato S, Aoyama T, Hayakawa Y, Kanoh M, Maruyama R, Arai M, Nishigaki K, Minatoguchi S, Fukuda K, Fujiwara T, Fujiwara H. Characterization of ultrastructure and its relation with DNA fragmentation in Fas-induced apoptosis of cultured cardiac myocytes. *J Pathol* 2001;193(4):546-556.
- 26 Fan D, Fan TJ. Clonidine induces apoptosis of human corneal epithelial cells through death receptors-mediated, mitochondria-dependent signaling pathway. *Toxicol Sci* 2017;156(1):252-260.
- 27 Wajant H. The Fas signaling pathway: more than a paradigm. *Science* 2002;296(5573):1635-1636.
- 28 Wyllie AH, Kerr JF, Currie AR. Cell death: the significance of apoptosis. *Int Rev Cytol* 1980;68:251-306.
- 29 Jin ZY, El-Deiry WS. Overview of cell death signaling pathways. *Cancer Biol Ther* 2005;4(2):139-163.
- 30 Adams JM, Cory S. The Bcl-2 protein family: arbiters of cell survival. *Science* 1998;281(5381):1322-1326.
- 31 Siddiqui WA, Ahad A, Ahsan H. The mystery of BCL2 family: Bcl-2 proteins and apoptosis: an update. *Arch Toxicol* 2015;89(3):289-317.
- 32 Youle RJ, Strasser A. The BCL-2 protein family: opposing activities that mediate cell death. *Nat Rev Mol Cell Biol* 2008;9(1):47-59.
- 33 Czabotar PE, Lessene G, Strasser A, Adams JM. Control of apoptosis by the BCL-2 protein family: implications for physiology and therapy. *Nat Rev Mol Cell Biol* 2014;15(1):49-63.
- 34 Brunelle JK, Letai A. Control of mitochondrial apoptosis by the Bcl-2 family. *J Cell Sci* 2009;122(Pt 4):437-441.
- 35 Fulda S. Caspase-8 in cancer biology and therapy. *Cancer Lett* 2009;281(2):128-133.